

Omni-directional Dielectric Mirrors

MASUD MANSURIPUR

An omni-directional dielectric mirror (also known as a one-dimensional photonic bandgap crystal)^{1,2} exhibits 100% reflectivity at all angles of incidence and for all states of incident polarization.^{3,4} Unlike metallic mirrors, which absorb a small fraction of the incident optical power, dielectric reflectors are lossless. These properties make omni-directional dielectric mirrors ideal candidates for applications in which a beam of light in an unknown or unpredictable polarization state is likely to arrive at the mirror from any direction, and in which loss of light at the mirror, no matter how small, is deemed intolerable. A good example is provided by the walls of an optical waveguide. Since there are numerous reflections from the walls as a beam of light travels through, even small losses at each encounter with a wall rapidly deplete the beam's energy.

A typical omni-directional reflector is a periodic stack of bilayers, each bilayer consisting of a high-index and a low-index dielectric layer. The larger are the refractive indices of the available dielectrics (and also the larger is the difference between these indices), the easier it is to design the reflector. For example, if the two materials available for fabricating a stack of bilayers have indices $n_1 = 1.5$ and $n_2 = 2.0$, it is impossible to obtain omni-directionality for both p- and s-polarized light. However, with $n_1 = 1.5$ and $n_2 = 2.3$, an omni-directional reflector can be designed. When the available dielectrics have reasonably large indices, it is also possible (by properly selecting the layer thicknesses) to achieve omni-directionality over a broad range of wavelengths.

In this article we describe a theory of omni-directional reflectors, and outline a method of selecting the layer thicknesses for a given pair of indices n_1, n_2 . Although the following discussions are confined to flat mirrors, it is clear that the exterior of a glass cylinder (or the interior of a hollow tube) may also be coated with

omni-directional reflectors. As long as the diameters of these cylinders/tubes are not too small (compared to the incident wavelength), the walls will appear flat locally and, therefore, the cylinder/tube may be used as an essentially lossless waveguide.⁴

General properties

Consider a periodic multilayer stack such as that depicted in Fig. 1. The stack consists of an infinite number of identical blocks, each block having reflection coefficients $r = |r| \exp(i\phi_r)$ from the top side and $r = |r| \exp(i\phi_r)$ from the bottom side, as well as transmission coefficient $t = |t| \exp(i\phi_t)$ from either side. In general, r, r , and t are functions of the incidence angle θ and the polarization state (p or s) of the incident light. From the reciprocal properties of electromagnetic waves in non-absorbing media it is known that t should be the same whether the incidence is from the top or from the bottom side, that $|r| = |r|$, and that $1/2(\phi_r + \phi_r) = \phi_t \pm 90^\circ$.⁵ Also, from conservation of energy, $|r|^2 + |t|^2 = 1$.

As shown in Fig. 1, one can express the reflection coefficient r_o from the top of the stack in terms of the parameters r, r, t of the individual blocks by assuming a diminishing air-gap between the top unit and the rest of the stack. Denoting the round-trip phase delay within this (artificial) air-gap by δ , and recognizing that the reflectivity r_o of the infinite stack is the same with and without its uppermost block, we write

$$\begin{aligned} r_o &= \lim_{\delta \rightarrow 0} \{ r + r_o t^2 \exp(i\delta) + r_o^2 r t^2 \exp(2i\delta) + r_o^3 r^2 t^2 \exp(3i\delta) + \dots \} \\ &= [r - r_o (r r - t^2)] / (1 - r_o r) \\ &= \{ r - r_o \exp[i(\phi_r + \phi_r)] \} / (1 - r_o r). \end{aligned} \tag{1}$$

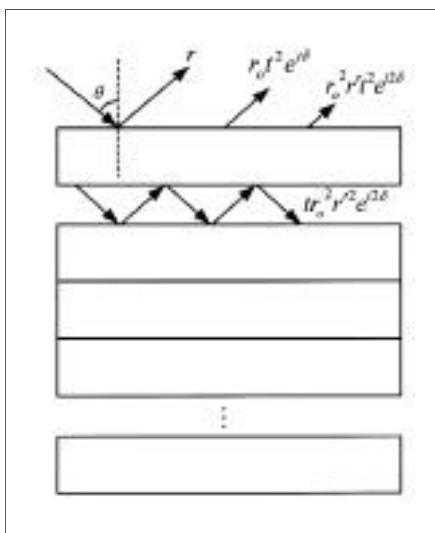


Figure 1. Method of calculating the reflection coefficient r_o of a periodic stack in terms of the parameters r, r, t of the individual blocks that comprise the stack.

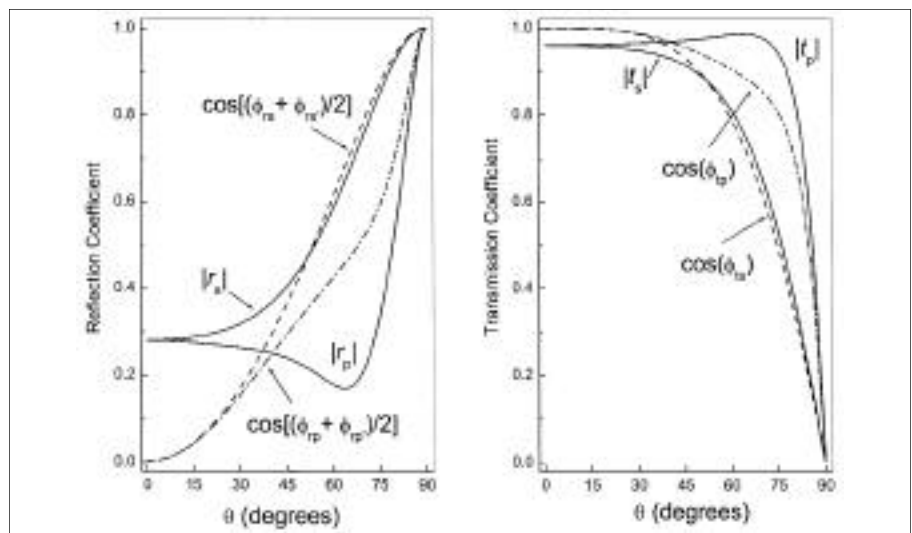


Figure 2. Plots of the various functions appearing in Ineqs. (3) for a bilayer consisting of a pair of dielectric layers, each having a quarter-wave thickness at the free-space wavelength of $\lambda_o = 633$ nm at normal incidence. ($n_1 = 2, t_1 = 79.0$ nm, $n_2 = 1.5, t_2 = 105.5$ nm.)

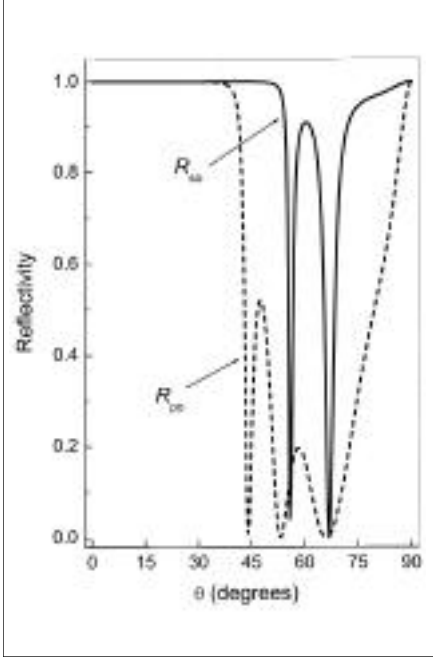


Figure 3. Computed reflectivity R versus θ for p- and s-polarized light for a quarter-wave stack consisting of twenty repetitions of the bilayer depicted in Fig. 2. R_{po} and R_{so} are $\sim 100\%$ in those regions where Ineqs. (3) are satisfied.

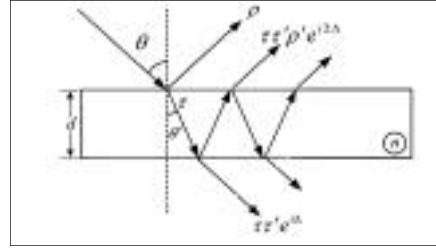


Figure 4. Method of calculating the reflection and transmission coefficients, r and t , for a single-layer dielectric slab of thickness d and refractive index n .

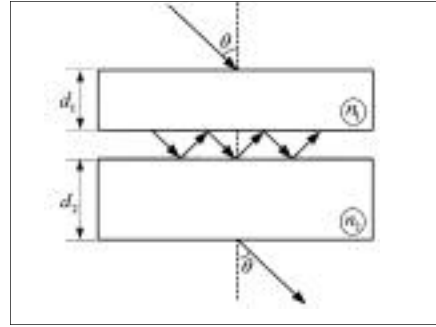


Figure 5. Method of calculating the transmission coefficient t of a bilayer slab consisting of two dielectric layers, one having thickness d_1 , index n_1 , the other having thickness d_2 , index n_2 .

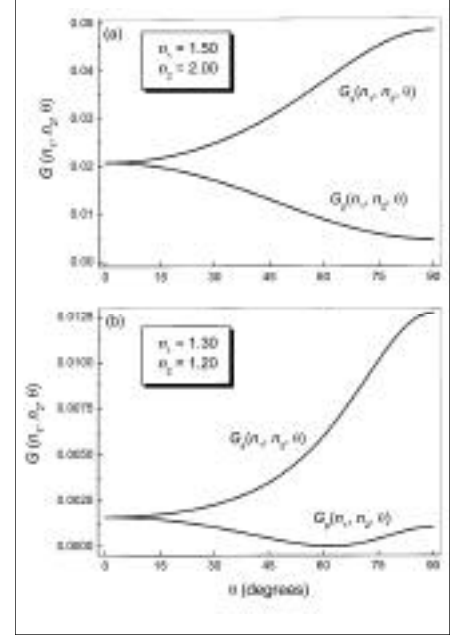


Figure 6. Plots of the functions $G_{ps}(n_1, n_2, \theta)$ versus θ for specific values of n_1, n_2 . In (a) n_1 and n_2 are large enough to satisfy Ineq. (13), thus ensuring that the Brewster angle is inaccessible from outside the stack. In (b) the Brewster angle is reached at $\theta = 61.9^\circ$.

The above formula is a quadratic equation in r_o . A 100% reflector requires that $|r_o| = 1$. Equation (1) then yields the following expression for the phase ϕ_o of r_o in terms of $|r|$, ϕ_r , ϕ_t :

$$\cos [\phi_o - 1/2 (\phi_r - \phi_t)] = \cos [1/2 (\phi_r + \phi_t)] / |r|. \quad (2)$$

Since in practice the actual value of ϕ_o is irrelevant, the above equation predicts that the reflectivity $R_o = |r_o|^2$ of the stack will be unity provided that the right-hand-side of Eq. (2) is confined to the interval $[-1, +1]$; in other words, the necessary and sufficient condition for the infinite dielectric stack of Fig. 1 to have 100% reflectivity may be written as follows:

$$|r| > |\cos [1/2 (\phi_r + \phi_t)]|. \quad (3a)$$

Using the identity $|r|^2 + |t|^2 = 1$ and the relation among ϕ_r , ϕ_t , ϕ_t mentioned earlier, Ineq. (3a) may be written in either of the following alternative forms:

$$|r| > |\sin \phi_t|, \quad (3b)$$

$$|t| < |\cos \phi_t|. \quad (3c)$$

The three inequalities (3a), (3b), and (3c) are equivalent and may be used interchangeably. As an example, consider a unit block consisting of a pair of high-index, low-index layers, each a quarter-wave thick at the free-space wavelength of $\lambda_o = 633$ nm at normal incidence (i.e., $\theta = 0$). Let $n_1 = 2.0$, $t_1 = 79.0$ nm, $n_2 = 1.5$, $t_2 = 105.5$ nm. Figure 2 shows plots of $|r|$ and $\cos [1/2 (\phi_r + \phi_t)]$ in frame (a), $|t|$ and $\cos \phi_t$ in frame (b), as functions of θ for both p- and s-polarized incident plane-waves.⁶ Note that In-

eqs. (3) are satisfied for p-light when $0 < \theta < 40^\circ$, and for s-light when $0 < \theta < 52^\circ$.

The computed p- and s-reflectivities for a quarter-wave stack consisting of twenty repetitions of the above bilayer are shown in Fig. 3.⁶ As expected, $R_{po} = |r_{po}|^2 = 1$ in the incidence range $0 < \theta < 40^\circ$, and similarly $R_{so} = |r_{so}|^2 = 1$ in the range $0 < \theta < 52^\circ$.

Single dielectric layer

In principle, the unit block from which an omni-directional reflector is constructed can be a bilayer or a multilayer, which may even contain gradient-index layers. It should be obvious that a single homogeneous layer (say, having index n and thickness d) will never produce a 100% reflector; therefore, Ineqs. (3) cannot be satisfied for such a layer. (We note in passing that for a single layer $\phi_r = \phi_t = \phi_t \pm 90^\circ$.)

Let us examine in some detail the single dielectric layer shown in Fig. 4. The monochromatic plane wave of wavelength λ_o is incident on the top surface of the layer at an angle θ ; the Fresnel reflection and transmission coefficients of the top surface are ρ and τ . Inside the layer the transmitted wave-vector makes an angle θ with the surface normal. The reflection and transmission coefficients at the bottom surface, where the light shines from within the slab onto the glass-air interface, are ρ and τ . Reciprocity may be invoked to show that, for both p- and s-polarization, $\rho = -\rho$ and $\rho^2 + \tau\tau = 1$ at all θ . The dependences of ρ on n and θ for p- and s-light are given by the Fresnel formulas⁷

$$\rho_p = (\overline{n^2 - \sin^2\theta} - n^2 \cos\theta) / (\overline{n^2 - \sin^2\theta} + n^2 \cos\theta), \quad (4a)$$

$$\rho_s = (\cos\theta - \overline{n^2 - \sin^2\theta}) / (\cos\theta + \overline{n^2 - \sin^2\theta}). \quad (4b)$$

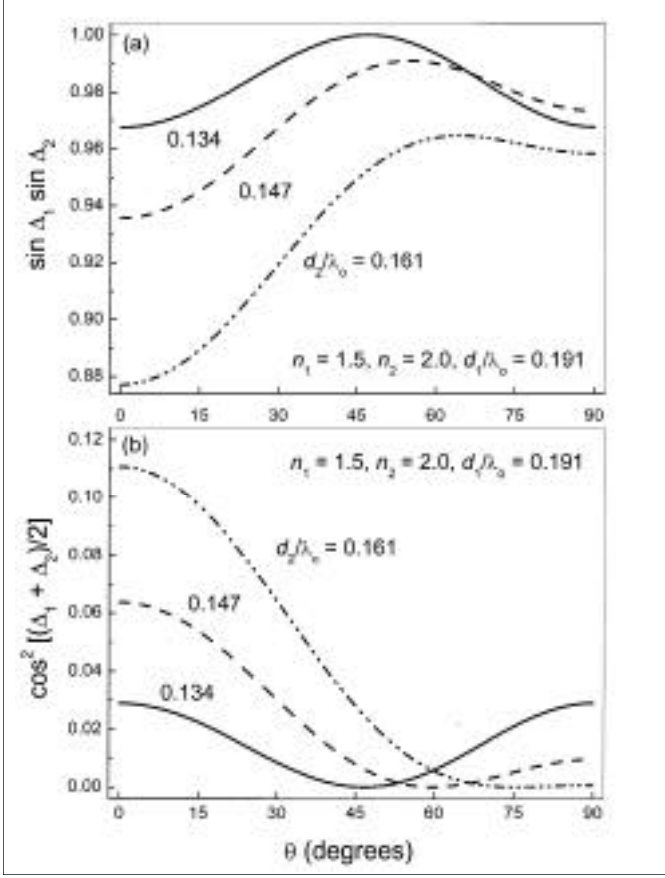


Figure 7. (a) Plots of $\sin \Delta_1 \sin \Delta_2$ versus θ for a bilayer slab consisting of materials with $n_1 = 1.5$ and $n_2 = 2.0$. The first layer's thickness is fixed at $d_1 = 0.191 \lambda_0$, but the second layer's assumes one of three different values. (b) Same as (a) for the function $\cos^2 [1/2(\Delta_1 + \Delta_2)]$.

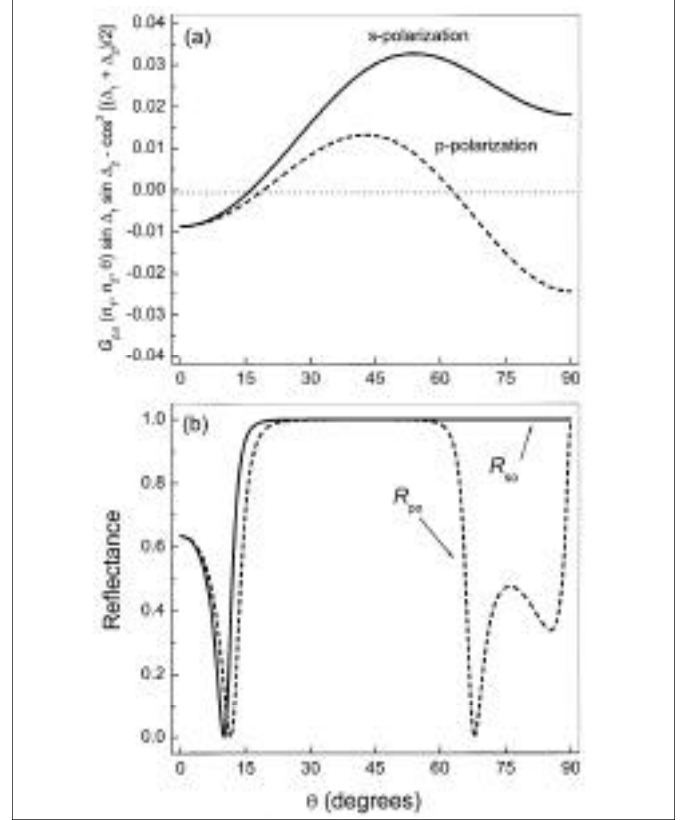


Figure 8. (a) Plots of $G_{ps}(n_1, n_2, \theta) \sin \Delta_1 \sin \Delta_2 - \cos^2 [1/2(\Delta_1 + \Delta_2)]$ versus θ for a bilayer having $n_1 = 1.5, d_1 = 0.191 \lambda_0$ and $n_2 = 2.0, d_2 = 0.134 \lambda_0$. At small angles of incidence both p- and s-light violate Ineq. (11a), while at large angles only p-light is inadequate. (b) Computed plots of p- and s-reflectivity, R_{ps}, R_{so} , versus θ for a twenty-period stack of the above bilayer. The regions of ~100% reflectivity coincide with those that satisfy Ineq. (11a).

Also, the single-path phase-shift Δ acquired through the thickness d of the slab is

$$\Delta = 2\pi (nd/\lambda_0) \cos \theta, \quad (4c)$$

where θ is the angle of the refracted ray.⁷ The slab's reflection and transmission coefficients, r and t , may be obtained by summing the infinite number of rays multiply reflected from its front and rear facets, namely,

$$r = \rho + \tau \tau \rho \exp(i2\Delta) + \tau \tau \rho^3 \exp(i4\Delta) + \dots, \quad (5)$$

$$t = \tau \tau \exp(i\Delta) + \tau \tau \rho^2 \exp(i3\Delta) + \tau \tau \rho^4 \exp(i5\Delta) + \dots. \quad (6)$$

When simplified, the above expressions yield,

$$|r| = 2(\rho \sin \Delta) / \sqrt{\rho^4 - 2\rho^2 \cos(2\Delta) + 1}, \quad (7a)$$

$$\phi_r = \arctan \{ (1 - \rho^2) / [(1 + \rho^2) \tan \Delta] \}; \quad (7b)$$

$$|t| = (1 - \rho^2) / \sqrt{\rho^4 - 2\rho^2 \cos(2\Delta) + 1}, \quad (8a)$$

$$\phi_t = \arctan \{ [(1 + \rho^2) \tan \Delta] / (1 - \rho^2) \}. \quad (8b)$$

Equations (7) and (8) readily confirm that $|r|^2 + |t|^2 = 1$, that $\phi_r = \phi_t \pm 90^\circ$, and that a single-layer slab does not satisfy Ineqs. (3).

Double layer

Next, consider the bilayer slab depicted in Fig. 5. The top layer has index n_1 , thickness d_1 , and reflection and transmission coefficients r_1, t_1 at the incidence angle θ . The corresponding parameters of the second layer are n_2, d_2, r_2, t_2 . To determine the bilayer's overall transmission coefficient t , we assume a small air gap between the two layers and proceed to sum the partial transmission coefficients. We find, in the limit of a vanishing gap,

$$t = t_1 t_2 + t_1 t_2 r_1 r_2 + t_1 t_2 r_1^2 r_2^2 + \dots = t_1 t_2 / (1 - r_1 r_2). \quad (9)$$

It is now easy to apply criterion (3c) to the bilayer's transmission coefficient given by Eq. (9), to determine the conditions under which an infinite stack of bilayers becomes a 100% reflector. Both the necessary and sufficient conditions turn out to be

$$|t_1| |t_2| \left| |r_1| |r_2| - \cos(\phi_{r1} + \phi_{r2}) \right|, \quad (10)$$

which is actually two distinct inequalities in one, depending on whether the absolute value on the right-hand side is that of a pos-

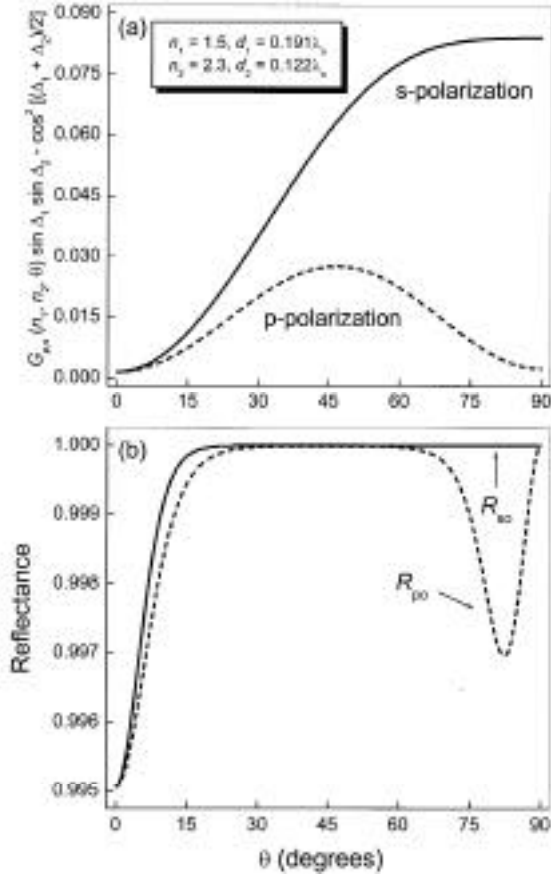


Figure 9. Same as Fig. 8 for a twenty-period stack consisting of layers with $n_1 = 1.5$, $d_1 = 0.191 \lambda_0$ and $n_2 = 2.3$, $d_2 = 0.122 \lambda_0$. It is seen in (a) that Ineq. (11a) holds for both polarization states throughout the entire range of incidence. In (b) the reflectances are $\sim 100\%$ everywhere. The slight drops in R_{po} and R_{so} are due to the fact that the assumed stack consists only of a finite number of bilayers; the reflectivity would rise rapidly if the total number of bilayers comprising the stack is increased. Note that the smaller the functions depicted in (a) become, the harder it is to obtain 100% reflectivity from a finite stack.

itive or a negative quantity. Substituting in Eq. (10) for r , t , ϕ in terms of ρ and Δ from Eqs. (7,8), we find the necessary and sufficient conditions for 100% reflectivity to be

$$G_{ps}(n_1, n_2, \theta) \sin \Delta_1 \sin \Delta_2 \cos^2 [1/2(\Delta_1 + \Delta_2)], \quad (11a)$$

$$G_{ps}(n_1, n_2, \theta) \sin \Delta_1 \sin \Delta_2 - \sin^2 [1/2(\Delta_1 + \Delta_2)], \quad (11b)$$

where,

$$G_{ps}(n_1, n_2, \theta) = (\rho_1 - \rho_2)^2 / [(1 - \rho_1^2)(1 - \rho_2^2)]. \quad (11c)$$

Inequalities 11(a, b) are the fundamental results of this paper, each expressing the condition (both necessary and sufficient) for the attainment of $R = 1$ from a periodic stack of bilayers. Whereas Ineq. (11a) leads to bilayer designs in which both layer thicknesses are close to $\lambda/4$, Ineq. (11b) yields structures in which one layer's thickness is $\sim \lambda/4$ while the other's is $\sim 3\lambda/4$.

Discussion

We begin by examining the behavior of $G_{ps}(n_1, n_2, \theta)$. According to Eq. (11c) this function depends only on ρ_1 and ρ_2 , which, in turn, are dependent on n_1 , n_2 , the angle of incidence θ , and the polarization state of the beam, but not on layer thicknesses d_1 , d_2 . For fixed values of n_1 , n_2 the function depends only on θ and on the polarization state. Substituting from Eqs. (4a) and (4b) into Eq. (11c) yields,

$$G_s(n_1, n_2, \theta) = 1/4 \frac{(n_1^2 - \sin^2 \theta) / (n_2^2 - \sin^2 \theta)}{(n_2^2 - \sin^2 \theta) / (n_1^2 - \sin^2 \theta) - 1/2}, \quad (12a)$$

$$G_p(n_1, n_2, \theta) = 1/4 \frac{(n_2/n_1)^2 (n_1^2 - \sin^2 \theta) / (n_2^2 - \sin^2 \theta)}{(n_1/n_2)^2 (n_2^2 - \sin^2 \theta) / (n_1^2 - \sin^2 \theta) - 1/2}. \quad (12b)$$

$G_{ps}(n_1, n_2, \theta)$ is plotted versus θ in Fig. 6 for both p- and s-polarized plane waves for the specific values (a) $n_1 = 1.5$, $n_2 = 2.0$, and (b) $n_1 = 1.3$, $n_2 = 1.2$. Although the selected values of n_1 , n_2 are specific, the shapes of the functions are quite general. The two functions for p- and s-light are always positive; they both start, at $\theta = 0^\circ$ (normal incidence), at the same level, from there G_s goes up and G_p down with increasing θ . The behavior shown in Fig. 6(a), where G_s increases while G_p decreases monotonically, is typical of situations of interest in this work, where the Brewster angle θ_B is inaccessible from outside the multilayer. The behavior depicted in Fig. 6(b), where G_s increases monotonically while G_p first drops to zero at θ_B ($\sim 61.9^\circ$ in this example) before rising again, is typical of situations where θ_B can be accessed from outside the stack. Since R_p at $\theta = \theta_B$ cannot be made equal to unity, the latter situation is of no interest here.

One can readily show that the slope of G_s versus θ is always positive. G_p , on the other hand, has a negative slope at $\theta = 0^\circ$, which continues to be negative up to where $\sin \theta = n_1^2 n_2^2 / (n_1^2 + n_2^2)$. At this point G_p reaches its minimum value of 0, then rises all the way until grazing incidence at $\theta = 90^\circ$. The angle θ at which G_p is a minimum corresponds to the Brewster angle θ_B between two media of indices n_1 and n_2 . When θ_B is accessible from the incidence medium (air in this case), it will be impossible to achieve 100% reflectivity at this particular angle. Therefore, we impose the following constraint on the indices of the bilayer:

$$(1/n_1)^2 + (1/n_2)^2 < 1. \quad (13)$$

In this way, $G_{ps}(n_1, n_2, \theta)$ will always exhibit the typical behavior depicted in Fig. 6(a), namely, both functions start at the same level, $1/4(n_1/n_2) + 1/4(n_2/n_1) - 1/2$, when $\theta = 0^\circ$. From there G_s increases and G_p decreases, both monotonically, with an increasing θ .

Inequality (11a) can be satisfied over the entire range of θ for both p- and s-light if Δ_1 and Δ_2 are maintained around $1/2\pi$ throughout the range $\theta = [0^\circ, 90^\circ]$. Likewise, Ineq. (11b) can be satisfied if Δ_1 is kept around $1/2\pi$ while Δ_2 is kept around $3\pi/2$ (or vice versa). When n_1 and n_2 are far apart, G_s and G_p will be fairly large, and choosing d_1 and d_2 to satisfy the requisite inequalities for all θ will not be difficult. When n_1 and n_2 are close together, however, it is easier to maintain Δ_1 and Δ_2 both around $1/2\pi$ (if at all possible), rather than to keep one of them around $3\pi/2$. This is simply because the variations with θ will be greater for that Δ which stays near $3\pi/2$. We limit the following discussion to stacks

that satisfy Ineq. (11a), but emphasize that a similar class of reflectors based entirely on Ineq. (11b) is feasible as well.

Selecting layer thicknesses

The parameters d_1 , d_2 should be chosen to satisfy Ineq. (11a) for all θ from 0 to 90°. Since $G_s > G_p$, one should try to achieve omnidirectional reflectivity for p-light only; the s-reflectivity will automatically follow suit.

The phase Δ acquired in a single path through a layer of thickness d and index n at incidence angle θ is given in Eq. (4c). Δ can be made equal to $1/2\pi$ at some arbitrary angle of incidence, say, $\theta = \theta_0$, by choosing the layer thickness d such that $nd\cos\theta_0 = d\sqrt{n^2 - \sin^2\theta_0} = 1/4\lambda_0$. Since θ can be anywhere between 0° and 90°, one should choose θ_0 in such a way as to make Δ vary symmetrically around $1/2\pi$. This is achieved when

$$d/\lambda_0 = 0.5/(n + \sqrt{n^2 - 1}). \quad (14)$$

The maximum deviation of Δ from $1/2\pi$ is then given by

$$|\Delta - 1/2\pi|_{\max} = 1/2\pi(1 - \sqrt{1 - n^{-2}}) / (1 + \sqrt{1 - n^{-2}}). \quad (15)$$

The expression on the right-hand side of Eq. (15) is a monotonically decreasing function of n , going from $1/2\pi$ to zero as n goes from 1 to ∞ . Therefore, the range of variation of Δ is smaller for larger values of n .

If d is chosen in accordance with Eq. (14), variations of Δ with θ will be symmetric around $\Delta = 1/2\pi$; as θ goes from 0 to 90°, Δ , which is larger than $1/2\pi$ in the beginning, drops to $1/2\pi$ then decreases further until its value at grazing incidence becomes equal to that at normal incidence. In this way, $\sin\Delta$ remains close to unity, swinging from just below +1 to +1 and then back to its initial value as the incidence goes from normal to grazing. Similarly, $\cos^2\Delta$ varies symmetrically around zero, moving, between normal and grazing incidence, from a small positive value to zero, then back again to its initial (positive) value. The choice of d according to Eq. (14) thus minimizes the swing of $\sin\Delta$ around its desired value of +1, while simultaneously minimizing the swing of $\cos^2\Delta$ around its desired value of zero.

In the case of a bilayer, one must select values for d_1 and d_2 ; both can be chosen to satisfy Eq. (14) with the corresponding value of n . In this way, Ineq. (11a) is likely to be satisfied, because $\sin\Delta_1 \sin\Delta_2$ will remain around unity, with a minimum swing throughout the range of θ , and, similarly, $\cos^2[1/2(\Delta_1 + \Delta_2)]$ remains around zero. Figure 7 shows plots of these functions for a bilayer consisting of materials with $n_1 = 1.5$, $n_2 = 2.0$. Layer thicknesses obtained from Eq. (14) are $d_1 = 0.191\lambda_0$ and $d_2 = 0.134\lambda_0$. With these choices, Fig. 7 shows that $\sin\Delta_1 \sin\Delta_2$ remains above 0.97 while $\cos^2[1/2(\Delta_1 + \Delta_2)]$ remains below 0.03 throughout the entire range of θ .

Unfortunately, the function $G_p(n_1, n_2, \theta)$ shown in Fig. 6(a) is extremely small, and the aforementioned choice of layer thicknesses is not able to yield a 100% reflector throughout the entire range of incidence. Because G_p is relatively large near normal incidence but decreases with an increasing θ , it may be helpful to make the curves of $\sin\Delta_1 \sin\Delta_2$ and $\cos^2[1/2(\Delta_1 + \Delta_2)]$ slightly asymmetric. This is done by choosing a somewhat larger thickness for layer 2, as shown in Fig. 7, where the broken curve corresponds to $d_2 = 0.147\lambda_0$ and the dotted curve to $d_2 = 0.161\lambda_0$.

(d_2 is a better choice for this purpose than d_1 , because the corresponding layer has a larger n and, therefore, its variation with θ is smaller, thus causing a smaller variation in the functions depicted in Fig. 7.) Note in Fig. 7 that as d_2 increases, at large θ , the function $\cos^2[1/2(\Delta_1 + \Delta_2)]$ is depressed, and the function $\sin\Delta_1 \sin\Delta_2$ moves toward unity (at least initially); both of these trends are helpful in satisfying Ineq. (11a). Unfortunately, the other side of the curves (i.e., the side around $\theta = 0^\circ$) moves in the wrong direction, making it harder to satisfy the inequality at and around normal incidence. All in all, it turns out that it is impossible to design an omnidirectional reflector with bilayers having $n_1 = 1.5$ and $n_2 = 2.0$.

Figure 8 shows the best that one can achieve with $n_1 = 1.5$, $n_2 = 2.0$, and layer thicknesses $d_1 = 0.191\lambda_0$, $d_2 = 0.134\lambda_0$ (chosen to satisfy Eq. (14)). Figure 8(a) shows plots of the function $G_{p,s}(n_1, n_2, \theta) \sin\Delta_1 \sin\Delta_2 - \cos^2[1/2(\Delta_1 + \Delta_2)]$ versus θ for both p- and s-polarized light; both functions must stay above zero to satisfy Ineq. (11a). Figure 8(b) shows computed plots of reflectivity, R_{p0} and R_{s0} , versus θ for a twenty-period stack of this bilayer.⁶ It is seen that ~100% reflectivity is achieved in exactly those regions where the functions plotted in Fig. 8(a) are positive-valued.

Designing an omnidirectional reflector

To achieve 100% reflectivity over the entire range of incidence requires materials with larger indices (or a larger index difference) than those examined above. For example, by keeping n_1 at 1.5 but raising n_2 to 2.3 it is possible to satisfy Ineq. (11a) with $d_1 = 0.191\lambda_0$ and $d_2 = 0.122\lambda_0$, as shown in Fig. 9. The plots in Fig. 9(a) confirm that Ineq. (11a) for both p- and s-light is satisfied over the entire range of incidence. Figure 9(b) shows plots of reflectivity versus θ for a twenty-period stack;⁶ both R_{p0} and R_{s0} are seen to be greater than 99.5% between normal and grazing incidence. To increase the reflectivity beyond 99.5% one should either increase the number of bilayers comprising the stack, or use materials which have a larger index difference.

Finally, it must be mentioned that omnidirectional reflection can be achieved not just for one wavelength but over a continuous range of wavelengths. To the extent that n_1 and n_2 remain constant over the desired range of λ , the functions G_p and G_s remain the same at all wavelengths of interest. Designing an omnidirectional reflector for a range of λ then reduces to choosing thicknesses d_1 and d_2 that satisfy Ineq. (11a) throughout that range. The techniques described in this article can be readily extended to allow adjusting layer thicknesses for the desired band of wavelengths.

References

1. E. Yablonovitch, Phys. Rev. Lett. **58**, 2059 (1987).
2. J. D. Joannopoulos, R. D. Meade, and J. N. Winn, *Photonic Crystals*, U. Princeton Press, Princeton, N.J., 1995.
3. J. N. Winn, Y. Fink, S. Fan, and J. D. Joannopoulos, Opt. Lett. **23**, 1573-5 (1998).
4. Y. Fink, J. N. Winn, S. Fan, C. Chen, J. Michel, J. D. Joannopoulos, and E. L. Thomas, Science **282**, 1679-82 (1998).
5. M. Mansuripur, Opt. & Phot. News **9**, (7) 53-8 (1998).
6. The computer simulations reported in this article were performed with MULTILAYER™, a product of MM Research, Inc., Tucson, Arizona.
7. M. Born and E. Wolf, *Principles of Optics*, 6th ed., Pergamon Press, Oxford, 1980.